Active Subwoofer System using Servo Control

by

Michael Kramer
Phil Schniter

April 27, 1992

ABSTRACT

This report describes the design and construction of an accelerometer-controlled active subwoofer system. A piezo-electronic element mounted on the woofer cone is used to tailor the frequency and transient responses of the subwoofer system and minimize distortion. A Proportional-Integral controller is used in the feedback loop of the system to accomplish these goals.

The system hardware consists of a 12 in driver mounted in a sealed box that is driven by a 120 W power amplifier. A separate box, containing the necessary control circuitry, also includes filters to separate the input signal into its high and low frequency components.

The system was designed to meet the specifications of a low frequency cutoff under 20Hz with a Q of 0.7. We required that the system's total harmonic distortion would be less than 5% at 30 W input power for frequencies above 30 Hz.

TABLE OF CONTENTS

1. INTRODUCTION

The biggest motivation in building a subwoofer system is the inherent incapability of normal two or three-way speaker systems to accurately reproduce the full audio spectrum. To make this claim, a speaker system must have a flat frequency response in the frequency range of 20Hz - 20kHz. Because the requirements placed on low frequency drivers are very different that those placed on high frequency drivers, it is advantagous to build a subwoofer, which is designed to play only the lowest of frequencies. Because the human ear is essentially nondirectional at frequencies below 100Hz, it is possible to cut costs in half by building a monaural subwoofer to be used with a pair of stereo satellite speakers.

In building subwoofers, one encounters certain compromises that can make the project expensive and extremely impractical. To extend frequency response down to 20Hz requires enormous boxes, large drivers and additional equalization [6]. Maintaining moderately good distortion figures at these frequencies mandates multiple large, expensive transducers. Most homes and studios do not have the room to support such huge structures, so a more practical design method is needed.

Our system uses a cone-mounted accelerometer to track the speaker's output and uses this information to keep itself on the path dictated by the input. This allows it to compensate for what would normally be nonideal frequency and transient responses and maintains superb distortion figures. The results are much less stringent demands on box size and driver costs, making our system a very practical one to use and own.

The reasons for trying to control the acceleration of our system rather than its position or velocity [10] are this: it can be shown that pressure, the mechanism by which the human ear perceives sound, is directly proportional to acceleration of the speaker cone [1]. By adjusting for a flat acceleration vs. frequency response, we ensure a flat pressure response.

One can get a better understanding of our system by looking at a simplified block diagram shown in Fig. 1.1. After input, the stereo signal is summed to mono before it is lowpass filtered. Once the signal makes its way through the amplifier, the sensor monitors the speaker cone movement

and sends this information to the controller. In our system, a Proportional-Integral (PI) controller was chosen for reasons which will be explained in Section 2.1. The control signal is then compared to the input signal by summing it in a negative feedback fashion, revealing any differences between the two. It can be seen that these differences will then be compensated for, as the new input to the amplifier will be, in effect, 'pre-warped'. One must remember that since the speed of the electronics is so much faster than the speeds at which the woofer is moving, all corrections will take place near instantaneously.

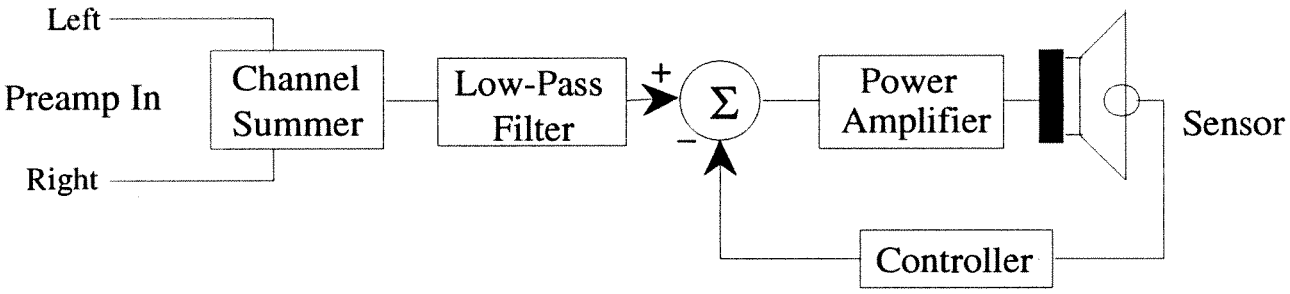

Figure 1.1. System Block Diagram

The performance specifications that are expected from our system are:

Frequency Response :	20Hz - 125Hz (±3dB)
Transient response :	Q = 0.7
Harmonic Distortion :	<5% at 1/4 power, 30-125Hz

2. DESIGN PROCEDURE

2.1 Controller Design

PI control was chosen mainly because it enables our system to independently achieve desired frequency and transient responses. There are two gains associated with this type of control, namely the proportional gain and the integral gain, and they can will be represented by the variables K_p and K_i, respectively. The transfer function of our controller can be represented in terms of the Laplace operator, 's', by:

$$G_c(s) = K_p + \frac{K_i}{s} = \frac{(K_p s + K_i)}{s} \tag{2.1.1}$$

The ideal pressure response of a sealed-box loudspeaker system should resemble a second-order highpass filter. This can be represented by:

$$G_p(s) = \frac{s^2}{s^2 + \left(\frac{\omega_n}{Q}\right) s + \omega_n^2} \tag{2.1.2}$$

In the above equation, the variable ω_n denotes the cutoff frequency in radians, and the variable Q denotes the quality factor. The closed-loop transfer function, with the controller placed in the feedback path, would be:

$$H(s) = \frac{G_p(s)}{1 + G_c(s)\, G_p(s)} \tag{2.1.3}$$

By substitution of equations (2.1.1) and (2.1.2) into (2.1.3) we can arrive at::

$$H(s) = \left[\frac{1}{K_p + 1}\right] \frac{s^2}{s^2 + \left[\frac{\frac{\omega_n}{Q} + K_i}{K_p + 1}\right] s + \left[\frac{\omega_n^2}{K_p + 1}\right]} \tag{2.1.4}$$

By inspection, the new cutoff frequency and system Q, denoted by primes, are then:

$$\omega_n' = \sqrt{\frac{\omega_n^2}{K_p + 1}} \tag{2.1.5}$$

$$Q' = \frac{\omega_n'(K_p + 1)}{\frac{\omega_n}{Q} + K_i} \tag{2.1.6}$$

Note that they are independently adjustable by the controller gains K_p and K_i. Also, note that the net gain of the transfer function is reduced. This will need to be compensated for in the final design.

Another control design that might accomplish the same task would be a pole-placement design using state-space methods. This was investigated in detail but was not chosen due to the complexity of its implementation and the fact that the associated gains approached 100 dB, which would have been very problematic in construction. In addition, it did not offer any inherent advantages over the PI control design.

2.2 Active Filter Design

The type of active filter network chosen to separate the audio spectrum between the subwoofer and the satellite speakers is commonly referred to as the Linkwitz-Riley network and has distinct advantages for audio use, the most important of these being that the outputs of the high- and low-pass sections sum to unity gain across the crossover region [3].

The fourth-order active filter is desirable in such applications because it provides a very steep rolloff, -24 dB/oct, while being fairly easy to implement. The basic transfer function of the Linkwitz-Riley fourth-order filter is simply two cascaded second-order Butterworth sections. The low-pass transfer function is shown below in Eq. (2.2.1) and the high-pass equivalent in Eq. (2.2.2) [3].

$$\frac{V_{in}}{V_{out}} = \frac{1}{s^2 + \sqrt{2}\, s + 1} \quad \frac{1}{s^2 + \sqrt{2}\, s + 1} \tag{2.2.1}$$

$$\frac{V_{in}}{V_{out}} = \frac{s^2}{s^2 + \sqrt{2}\, s + 1} \quad \frac{s^2}{s^2 + \sqrt{2}\, s + 1} \tag{2.2.2}$$

Summing these two and simplifying yields Eq. (2.2.3).

$$\frac{s^2 - \sqrt{2}\, s + 1}{s^2 + \sqrt{2}\, s + 1} \tag{2.2.3}$$

It is easy to see that the magnitude of all-pass response is equal to one for all frequencies, as shown in Fig. 2.2.1.

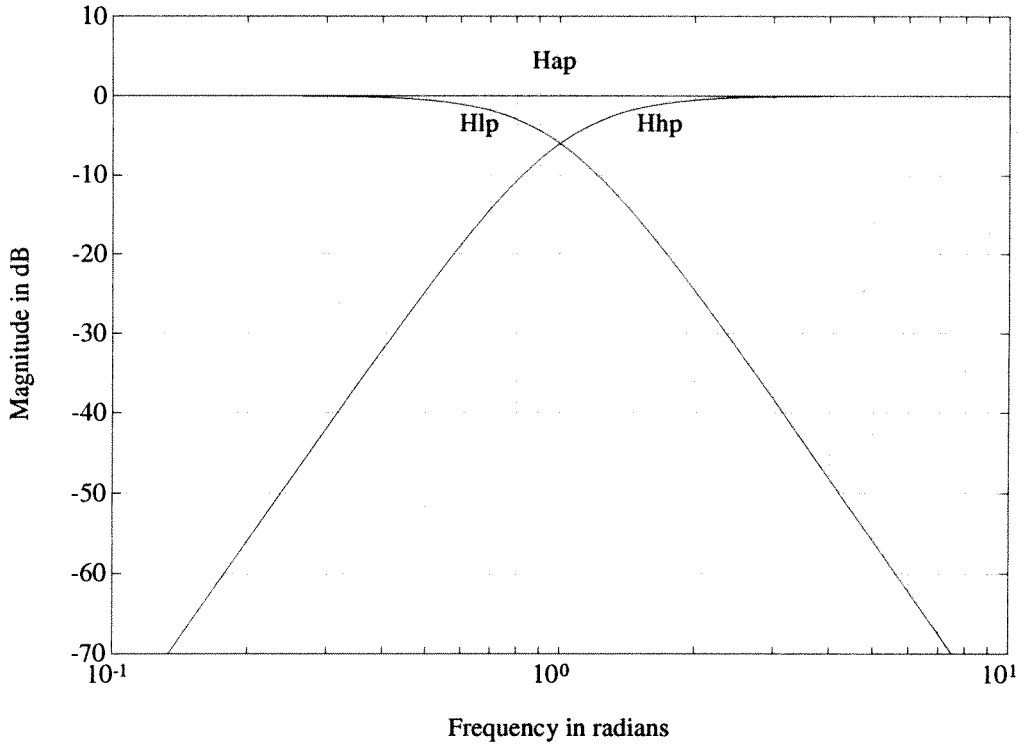

Fig. 2.2.1. Normalized response of low-pass (Hlp), high-pass (Hhp), and summed all-pass response (Hap)

The other major advantages to the fourth-order Linkwitz-Riley network lie in its phase characteristics. Being fourth-order, the phase is 0° and 360° for the low- and high-pass sections, respectively, at frequencies below cutoff. For frequencies far above cutoff, the phase is -360° and 0° for the low- and high-pass sections, respectively. Because the human ear cannot perceive a 360° phase difference, the phase response is audibly the same for frequencies outside the crossover region, as shown in Fig. 2.2.2.

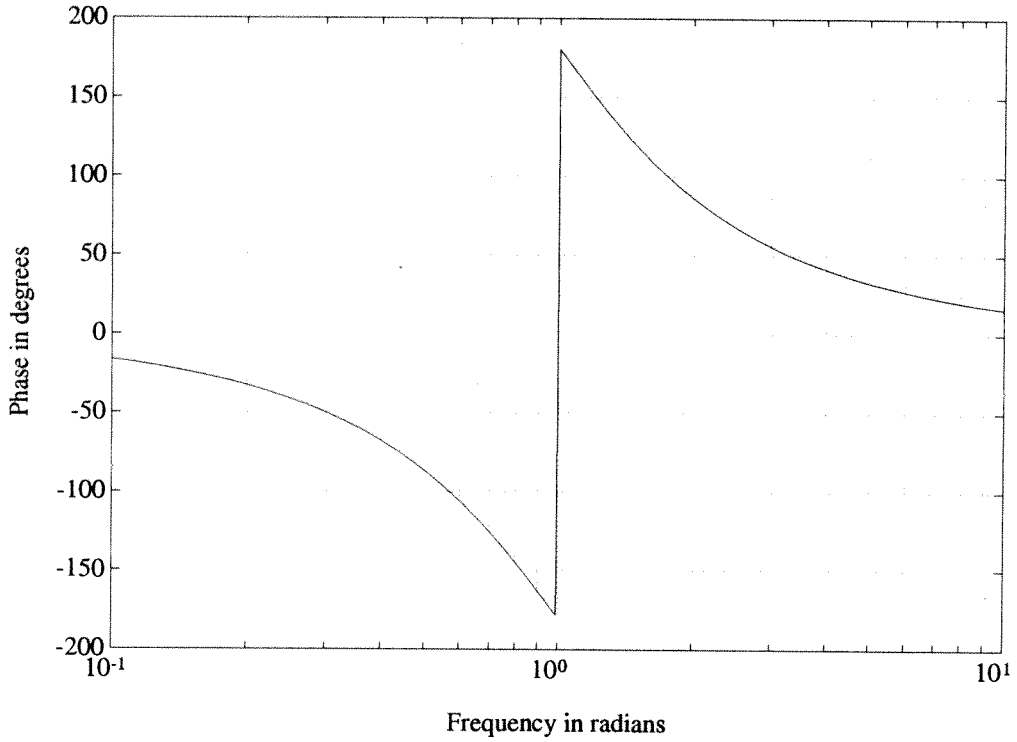

Fig. 2.2.2: Phase response for both low- and high-pass filters, as well as the summed all-pass response.

The biggest advantage of the Linkwitz-Riley filter is that it maintains a constant phase difference of 360° degrees between low- and high-pass sections throughout the crossover region. This can also be seen in Fig. 2.2.2.

The Linkwitz-Riley filter is especially suited for applications such as subwoofers, where the distance between drivers is not small compared to the wavelength of the crossover frequency. In

such cases, pressure level interferences between the drivers can cause audible distortion, resulting in poor depth perception and localization. Linkwitz-Riley filters have been shown to be "optimum" with respect to minimizing such distortion [8].

2.3 General System Design Procedure

The general design procedure was as follows. First, the uncontrolled system had to be finished so that it could be tested and the initial system parameters determined. These parameters determined the control gains as in discussed in Section 2.1. Next, the sensor was measured and compared to the SPL to guarantee that it was linear in the desired operating range. In addition, the sensor's resonant behavior was investigated.

Once the necessary information had been obtained, simulations of the design were needed to verify its performance and stability. Effects of additional phase delay and sensor resonance were important here in the stability and overall performance of the closed-loop system. In our case, the filters needed to suppress resonances were designed and optimized at this point.

When the simulation results indicated that the design would work, the controller electronics and necessary protection circuits were built, and each individual stage was tested to verify that it was working correctly. It was then time to close the loop and begin preliminary tests of the controlled system.

When all details such as ground-loop hum problems and noise interference had been taken care of, the system was tested with electronic measurement gear and general listening. Since then, possible improvements on later models of the system have been discussed.

3. DESIGN DETAILS

3.1 Design of the Uncontrolled Subwoofer System

The subwoofer system was built around a 12 in driver made by Audio Concepts, LaCrosse, WI. The driver was picked for its high excursion, high power handling and reasonable cost. In addition, its parameters indicated that it would mate well with a sealed box and it had a rigid dustcap providing a good sensor mounting location. Table 3.2.1 gives some of the relevant specifications given by the manufacturer.

TABLE 3.1.1 AC12 - MANUFACTURERS SPECIFICATIONS

Impedance	8 ohms
RMS Power	150 W
System Power	200 W
Sensitivity	90 dB (1W @ 1m)
X_{max}	8 mm
f_s	20 Hz
Q_{ms}	3.96
Q_{ts}	0.376
Q_{es}	0.416
M_{md}	79 g
Price	$65.00

The driver should be work well in a sealed box enclosure due to its Efficiency Bandwidth Product (E.B.P.). This is given in by Dickason [5] as:

$$\text{E.B.P.} = \frac{f_s}{Q_{es}} \tag{3.2.1}$$

Values for the E.B.P. in the range of 50 and below indicate that a closed box is suitable, while those above 100 suggest a vented box. The manufacturer recommended a closed box with suggested size between 2.5 and 5.0 cubic ft. The specifications above result in an E.B.P. of 48.1, verifying the recommendation.

To mate well with its crossover, a Zobel network was installed. It consists of a resistance and a capacitance (in series) placed in parallel with the woofer, and it effect is to counteract the rising voice coil impedance at higher frequencies due to the woofers inductance. This has the effect of making the woofer more closely approximate a resistive load, a characteristic which crossover network designs always assume.

The box was constructed around an approximate volume of 3.5 cubic ft. The dimensions were chosen around a ratio of 1.59:1.26:1, one of the 'golden ratios' to minimize unwanted intermal resonances [5]. The final inside dimensions (in inches) were $23 \times 18 \times 14.5$, which resulted in an internal box volume of 3.47 cubic ft.

Additional protections were taken against unwanted cabinet vibrations. First, corner braces were placed at every wall junction and additional cross braces were placed parallel and perpendicular to the woofer axis. Secondly, the inside cabinet walls were lined with a high density rubber material that acts to dissipate energy stored in cabinet resonances. Lastly, the interior of the box was stuffed with a fiber-like material resembling Dacron. This serves two purposes, the obvious one being a suppressor of internal reflections, and the other being an increase in effective box volume. More specifically, it changes the box compliance by transforming the interior thermodynamically, from an adiabatic to an isothermal system. The results are theoretical increases in box volume of 40%, and practical increases of 15% - 25% [5].

The box itself was constructed out of 3/4 in solid plywood, birch veneered on the outside. This was chosen over a heavier material such as MDF with the intention of minimizing the uncontrollable low-frequency resonances that a heavier materials would tend to exhibit. By moving box resonances up in frequency and efficiently damping them, we end up with resonances that carry less energy and ring for a shorter duration, and that are farther from the range in which the subwoofer is operating.

The box was glued and screwed, then all edges were routed. Any possible air leaks on the inside and outside of the box were sealed with a silicone sealant to prevent deviation from an ideal second-order system.

The sensor was mounted on the center of the hard plastic dustcap with epoxy. Pinholes were

punched in the woofer to permit the sensor leads to enter the subwoofer cabinet's interior. A small terminal strip was mounted on the woofer basket to permit the soldering of the sensor leads to the sensor cable, for which a 1/4 in stereo plug is provided on the input terminal plate on the subwoofer. A stereo plug was chosen for necessary isolation between the two signal carrying leads and the outer conductor, which inevitably touches chassis and can lead to ground loops. The mass of the sensor was small enough that the effects of mounting it on the speaker would be negligible [9].

The amplifier chosen to drive the system was a mono 120 W model using complementary MOSFET output devices. It was chosen on the basis of low distortion, wide frequency response, and adequate power for its low price. The amplifier was built from a kit and designed by S.M.E. Ltd., Honk Kong.

3.2 Calculation of Component Values

The basic circuits used to implement the low- and high-pass second-order sections are shown in Fig. 3.2.1 [3],

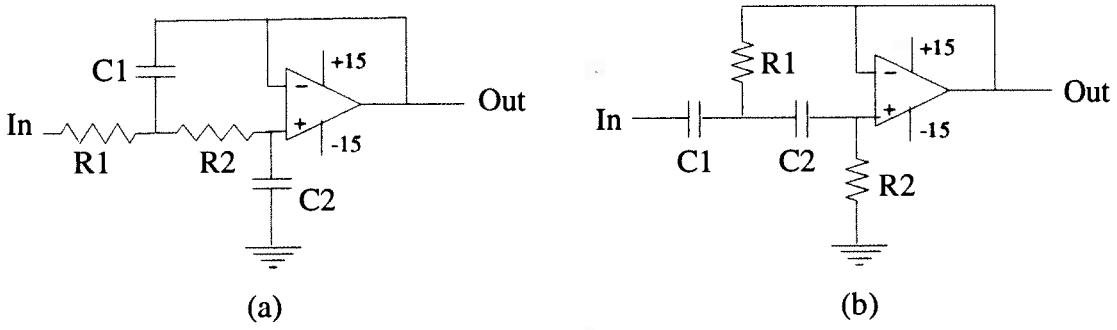

Fig. 3.2.1: Circuit design to implement second-order filter section.
(a) second-order low-pass section
(b) second-order high-pass section

and the transfer function in terms of the component values are given in Eqs. (3.2.1) and (3.2.2) for the low- and high-pass circuits, respectively.

$$\frac{1}{s^2(C_1C_2R_1R_2) + s[C_2(R_1+R_2)] + 1} \tag{3.2.1}$$

$$\frac{s^2(C_1C_2R_1R_2)}{s^2(C_1C_2R_1R_2) + s[R_1(C_1+C_2)] + 1} \tag{3.2.2}$$

Setting these transfer functions equal to the general form of second-order low- and high-pass transfer functions,

$$\frac{1}{\left(\frac{s}{\omega_n}\right)^2 + \left(\frac{s}{Q\omega_n}\right) + 1} \tag{3.2.3}$$

$$\frac{\left(\frac{s}{\omega_n}\right)^2}{\left(\frac{s}{\omega_n}\right)^2 + \left(\frac{s}{Q\omega_n}\right) + 1} \tag{3.2.4}$$

yields the following equations expressing the component values in terms of the desired Q and ω_n for the low-pass sections,

$$\frac{1}{Q\omega_n} = C_2(R_1+R_2) \tag{3.2.5}$$

$$\frac{1}{\omega_n^2} = C_1C_2R_1R_2 \tag{3.2.6}$$

and similarly for the high-pass sections.

$$\frac{1}{Q\omega_n} = R_1(C_1+C_2) \tag{3.2.7}$$

$$\frac{1}{\omega_n^2} = C_1C_2R_1R_2 \tag{3.2.8}$$

It was decided to cut the response of the subwoofer off at 125 Hz, and therefore the corresponding values of Q = .707, and $\omega_n = 2\pi*(125\text{ Hz})$ were used in the above equations. The component values for the low- and high-pass Linkwitz-Riley filters were calculated, and are given in Appendix 2. These are shown as R4-R7 and C1-C4 in Fig. A1.1 for the low-pass

sections, and as R29-R36 and C9-C16 in Fig. A1.2 for the high-pass sections.

To calculate the control gains, K_p and K_i, a short Matlab routine was written to simulate the entire closed loop system with different values of these parameters. Because of certain nonlinearities in the system, the equations given, Eqs. (2.1.5) and (2.1.6) could not be used to precisely achieve the exact K_p and K_i, but did give fairly accurate starting points. With these starting points, the values of K_p and K_i were tweaked until the desired response was achieved. The final values settled upon were $K_p = 3.202$ and $K_i = 290.7$. The Matlab code also took into account the natural gain of the integrator, about 147, and then calculated the required values for the summing input gain resistors with respect to a summing feedback resistor of 10 kΩ. Figure 3.2.2 shows both the desired response and the simulated response with these control values.

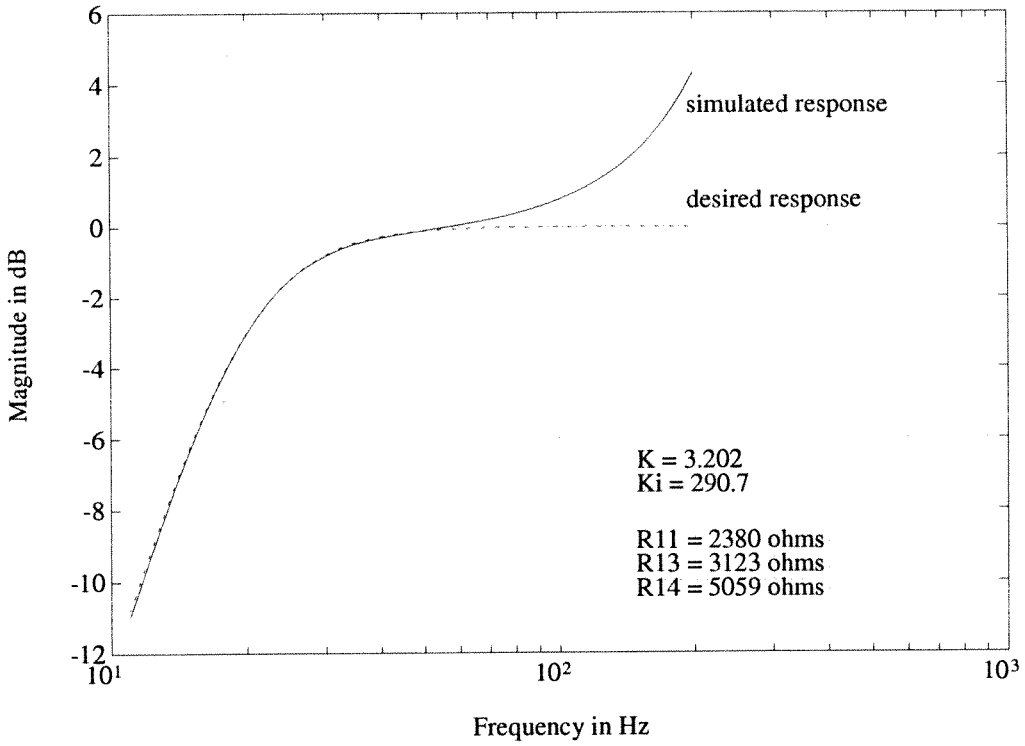

Fig. 3.2.2: Desired and Matlab simulated responses.

The hump toward the end of the simulated response is primarily due to the added resonance reduction filter at 150 Hz (discussed in 3.3). This was not a problem, since the input low-pass filter cuts off early enough to reduce this hump to an audibly negligible amount. (Figure 4.1.2 verifies that the error due to the hump is barely detectable.)

Our circuit design also incorporated the possibility of altering the frequency and transient response characteristics of the closed loop system. The resistors used for R11, R13, and R14 in Fig. A1.1 are mounted on a sixteen pin carrier, and by simply building a new carrier with the appropriate resistance values, nearly any response characteristics can be achieved.

3.3 Sensor Details

The choice for the specific accelerometer to use was based on a paper by Arthur Brown [2]. In his article, Brown attempts a similar arrangement using an accelerometer as a sensor. For reasons of cost, he chose a piezo-electric element from a piezo tweeter. Our final design used the piezo element from a Radio Shack tweeter, part no. 40-1937.

The piezo-electric element was removed and mounted onto the dust cap of the speaker cone as discussed in Section 3.1. The response of the sensor was measured along with the actual SPL and the results are shown in Fig. 3.3.1.

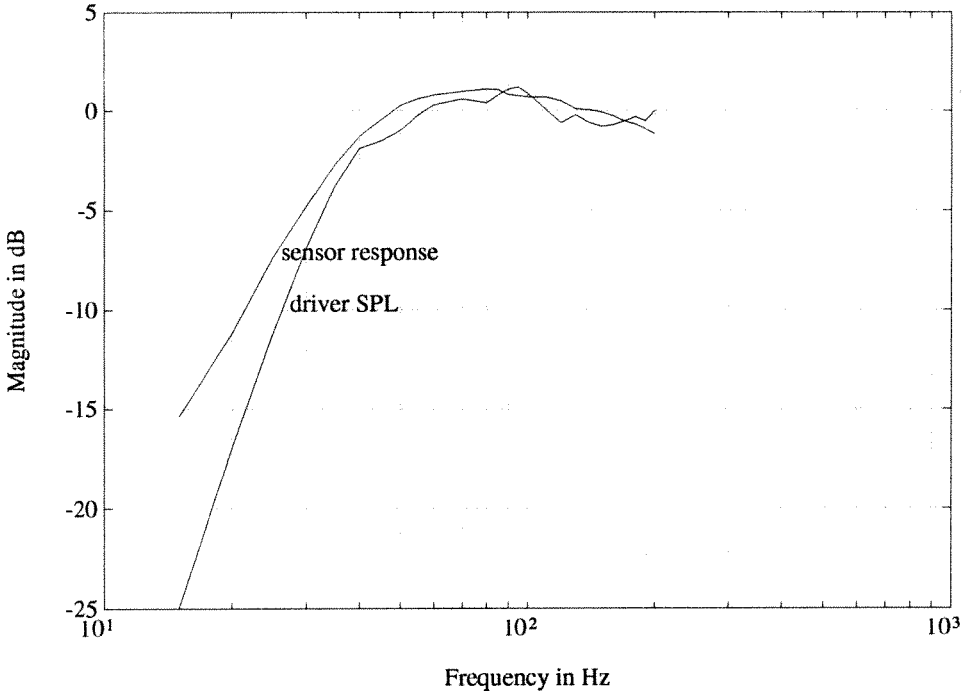

Fig. 3.3.1: Measured response data for both the sensor and driver SPL.

The error below rolloff between the sensor and SPL response is due to a pole in the actual SPL meter's transfer function occuring around 19 Hz. Compensating for this fact, the sensor response was found to be correct with respect to SPL across the desired system bandwidth, 20-200 Hz, within ± 1.2 dB, as shown in Fig. 3.3.2.

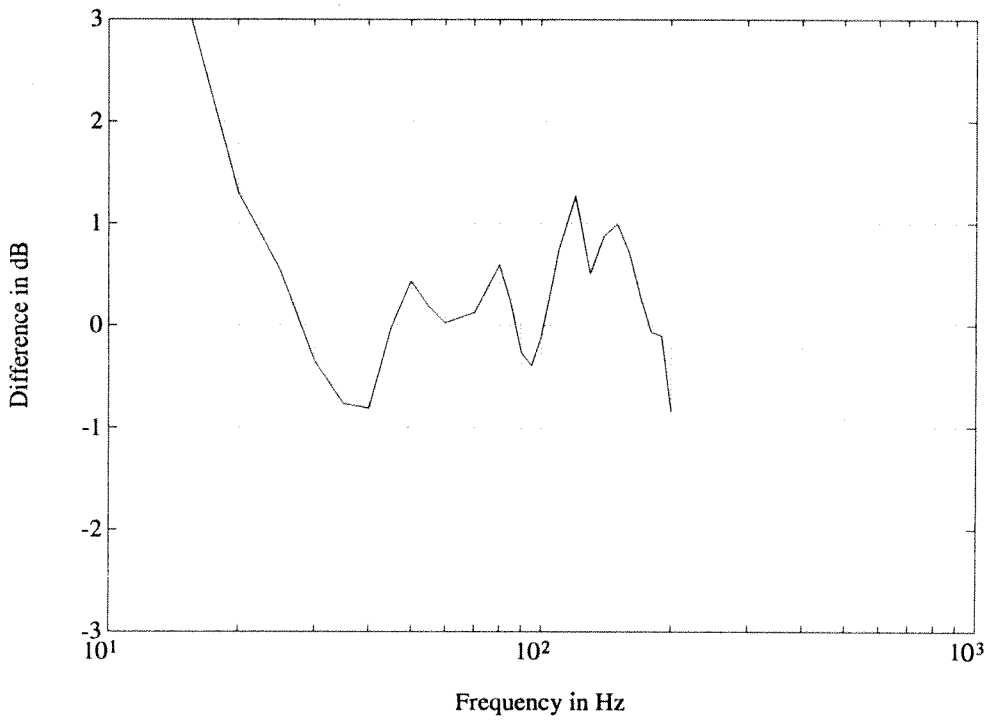

Fig. 3.3.2: Difference between actual driver SPL and measured sensor response.

Because ± 1.2 dB is nearly inaudible, it could be assumed then that the sensor was tracking the the SPL as expected, and the next problem to address was the sensor's physical resonance. Brown [2] found that his sensor resonance was fairly sharp and centered around 1000 Hz, while measurements of our sensor response in the resonance region were quite different. As can be seen in the magnitude plot of Fig. 3.3.3, the sensor had one distinct resonance closer to 900Hz, which begins affecting the linear response below 400 Hz, and showed a second prominent peak near 1500 Hz.

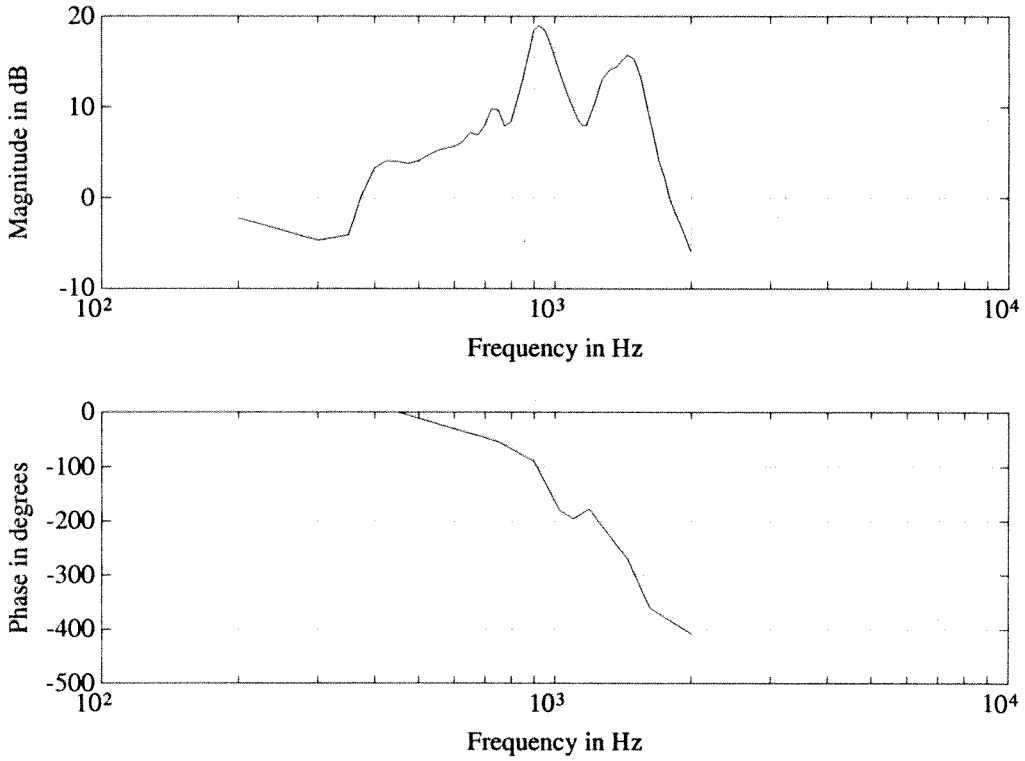

Fig. 3.3.3: Bode plots, both magnitude and phase, of raw sensor response.

Combined with the phase of the resonance, the results violate the gain and phase margin relationships of feedback in that the magnitude of the response is greater than 0 dB where the phase is -180°. This indicates positive feedback, rather than negative feedback, and results in closed-loop instablility.

To compensate for this problem, some sort of resonance reduction filter was required. Matlab simulations were run to tailor the net loop transfer function, which included the sensor resonance response, the PI controller, and a resonance attenuation filter. After several simulations, the filter decided on was a second-order low-pass filter with a Q=1, and f_c=150 Hz. The resulting magnitude and phase responses are shown in Fig. 3.3.4.

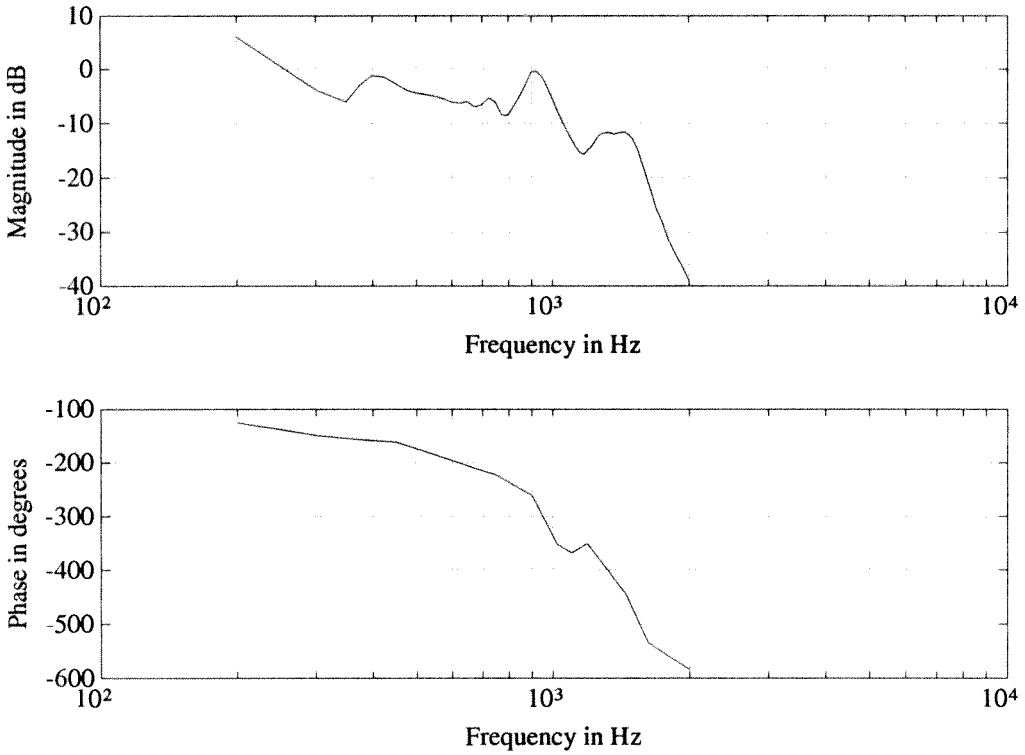

Fig. 3.3.4: Bode plots, both magnitude and phase responses, for entire loop, including P.I. controller, and 150 Hz low-pass filter.

The main compromise in designing this filter had to do with the problem of excess phase appearing in the passband. Higher order filters contributed more unwanted phase to the passband of the sysem and resulted in closed-loop transfer functions with rising magnitude responses over 100 Hz (see Fig. 3.2.2). Lower order filters did not provide enough resonance attenuation for the values of the loop gains that were required.

A Nyquist plot is also given to better see that the gain and phase margins are well within acceptable limits, shown in Fig. 3.3.5.

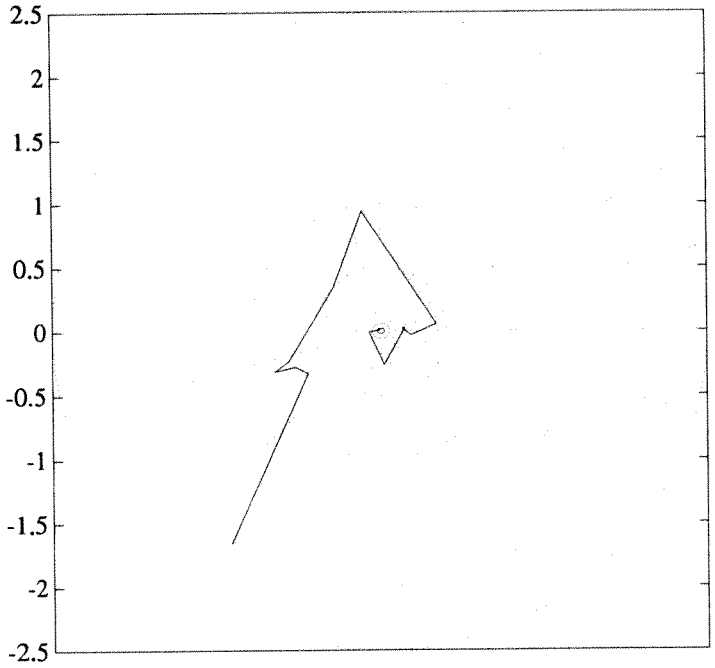

Fig. 3.3.5: Nyquist plot of entire loop, including P.I. controller and 150 Hz low-pass filter.

Note that the plot in Fig. 3.3.5 is linear (not dB) and that at -180°, the gain margin is approximately 1.667 (4.44 dB). The phase margin is about 45°.

The mentioned low-pass filter was constructed in the same fashion as the Linkwitz-Riley filters, with the exception of different Q and ω_n values of Q=1 and $\omega_n = 2\pi*(150\ Hz)$. Using Eqs. (3.2.5) and (3.2.6), as refrenced to Fig. 3.2.1(a), the appropriate values were computed and are included as R17, R18, C5, and C6 in the table in Appendix 2, and are shown in Fig. A1.1.

The sensor input is first buffered by $A5_1$, and R19 is included to compensate for internal capacitance of the sensor [2]. Following the buffer is an attenuator, for the actual sensor output was approximately 33% more than the amplifier input. The gain on this amplifier was set 0.75 to insure that the net transfer function, from input to amplifier to input to controller, had a gain of one at high frequencies .

3.4 Additional Circuitry

Due to the possibility of the feedback cable being removed accidentally, some sort of protection circuitry was a necessity. If the feedback cable is disconnected, it will cause two serious problems, the first being an increase in gain by a factor of (K_P + 1), normally on the order of 4. The other problem with removing the feedback cable lies in the fact that the sensor input would not be grounded, and instead would be floating and very succeptible to noise and hum. In fact, it was found to result in large dc voltages which could destroy the input stages of the amplifier.

This problem was solved by placing a relay in the signal path (see Fig. A1.1) directly before the output to the amplifier that would switch the output signal between the controlled and uncontrolled signal paths. By mounting a roller switch to sense the presence of the plug on the feedback cord, it was possible to have the entire control circuitry switched out of the signal path in the event that the sensor feedback cable is physically removed. A manual switch selecting between controlled and uncontrolled system operation was combined with the protection circuit, as was an LED indicating the mode of operation. The switching circuit was powered by a separate power supply as shown in Fig. A1.1, to avoid corruption of the audio power supply.

In addition to the relay protection circuit, a zener limiter [7] was incorporated into the summer by means of diodes D1 and D2 and a trimpot, R15, to adjust the hardness of clipping. This was included as a protection against abnormally high input levels which could damage the amplifier and speaker.

A dc blocking capacitor (C7 in Fig. A1.1) was introduced before the integrator to avoid the problem of infinite integrator gain of small dc offsets.

Other circuit stages include a left and right channel signal summer via R1, R2, and R3, as well as a bass volume control via a 100 kΩ potentiometer, R3. The left and right preamp signals are first buffered ($A1_1$ and $A1_2$ in Fig. A1.1), for any signal leakage between the left and right channels would result in poor stereo imaging. An additional amplifier ($A3_1$ in Fig. A1.1) is included just before the summing stage to provide for an extra margin of bass volume in the case that the satellite system is more sensitive than the subwoofer system.

4. DESIGN VERIFICATION

4.1 Frequency Response Measurements

Frequency response measurements were measured by tapping the sensor signal after the sensor input buffer, and measuring the gain in dB on a multimeter. Verified by comparisons between SPL and sensor data, our sensor is known to be linear throughout the frequency range that we are concerned with. Frequency samples were taken at closely spaced intervals, and the results are shown below for the uncontrolled response, Fig. 4.1.1, as well as the controlled response, Fig. 4.1.2.

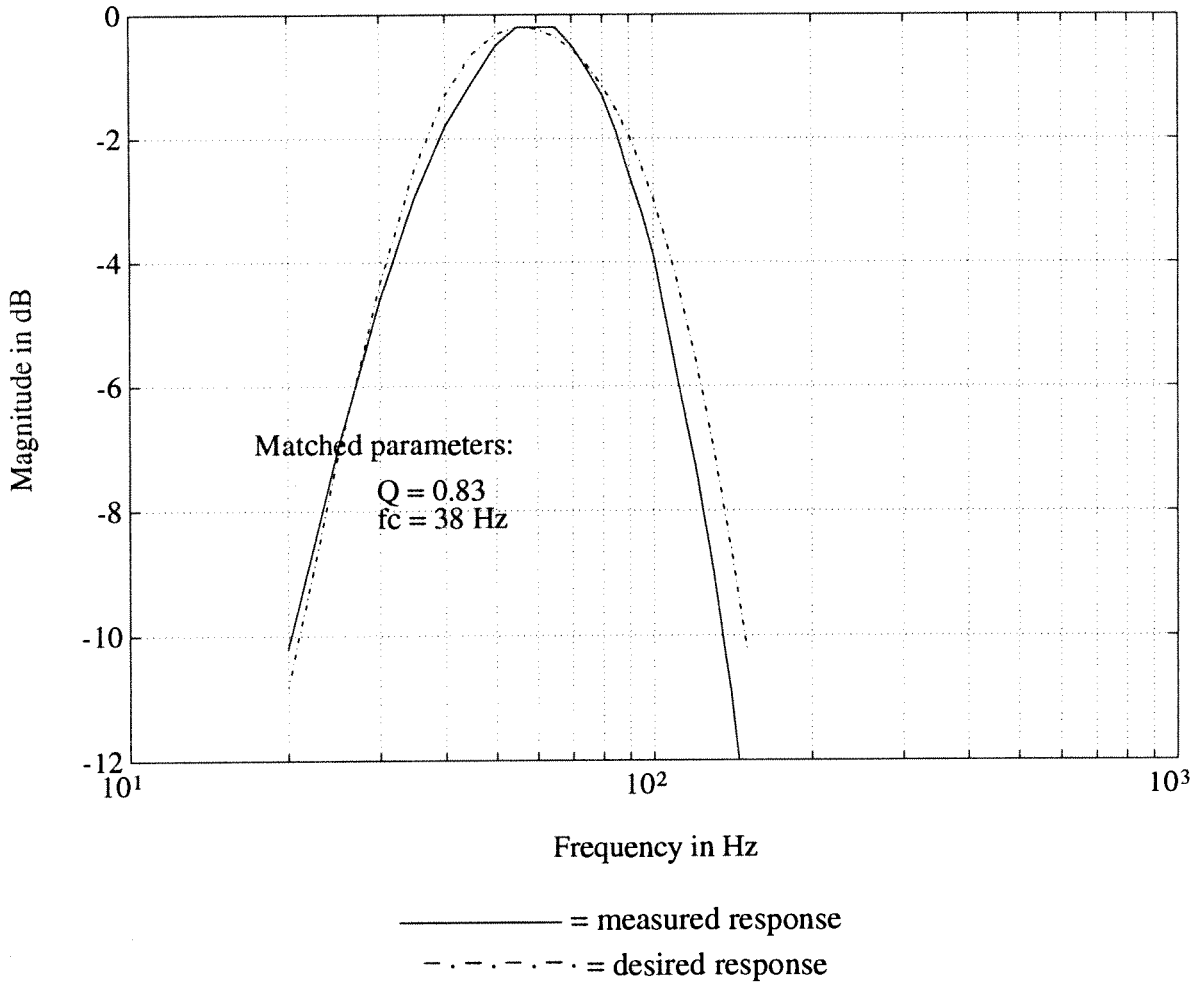

Fig. 4.1.1: Measured and desired frequency response for uncontrolled system.

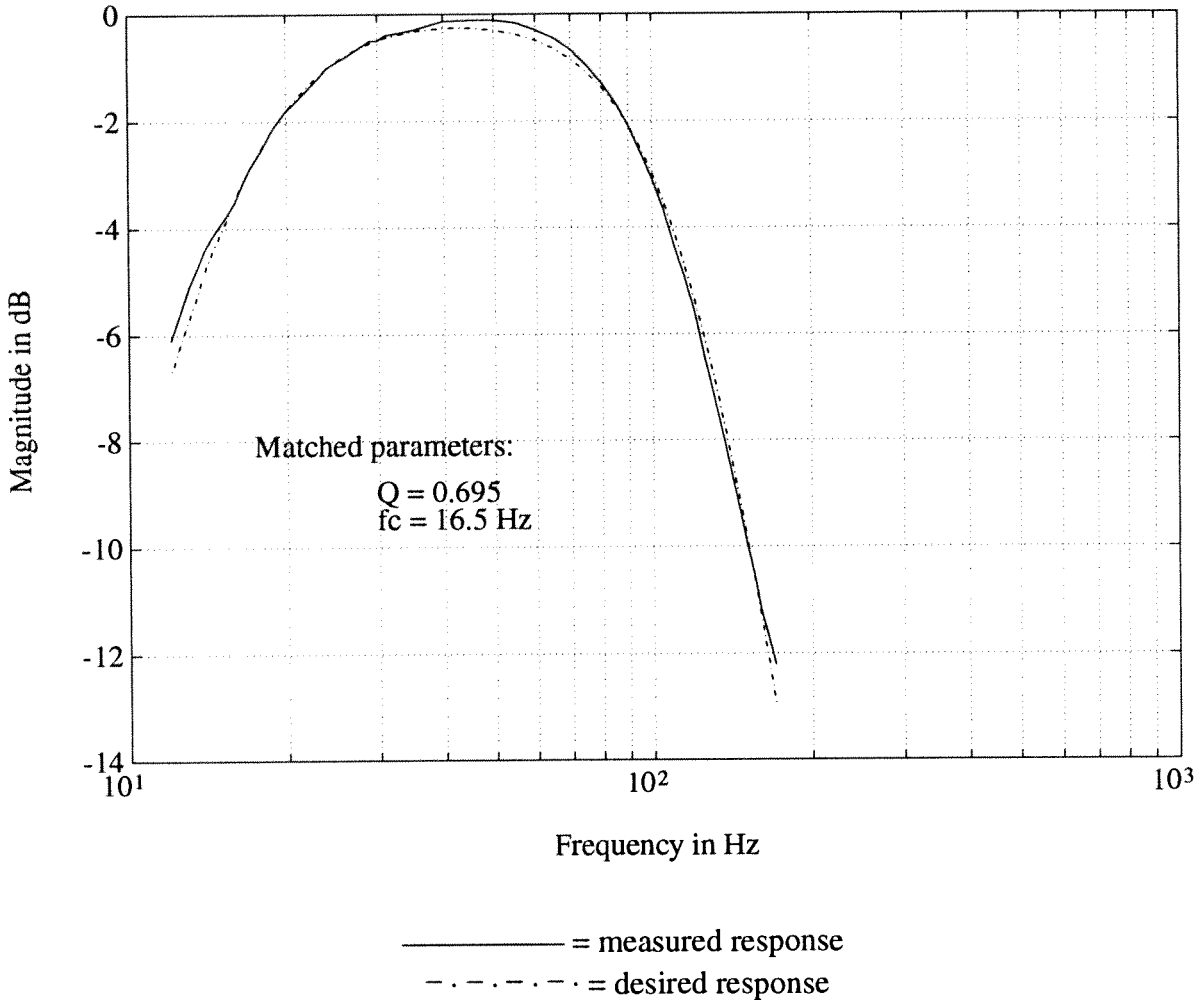

Fig. 4.1.2: Measured and desired frequency response for controlled system.

It should be noted that the cutoff of 16.5 Hz was under the predicted value of 20 Hz. This is due to our driver parameters changing slightly during the course of the design process.

4.2 Harmonic Distortion Measurements

The levels of harmonic distortion were measured using a NeXT computer, an A/D64x analog to digital converter and sound analysis programs developed at the Computer Music Project of the

University of Illinois. A function generator supplied a sine wave to the system inputs, and output for analysis was taken from the buffered sensor signal. Only the first eight harmonics are shown because the levels of higher harmonic components are negligible.

Table 4.2.1 contains the percentages of the total signal that each harmonic is responsible for at quarter power output levels with and without feedback. In the case of no measureable distortion, the fundamental, or first harmonic, would represent 100% of the signal. Values of less than .1% are represented by a dash.

TABLE 4.2.1 HARMONIC LEVELS AT 1/4 POWER OUTPUT

without feedback:

freq.	#1	#2	#3	#4	#5	#6	#7	#8
20 Hz	70.4%	7.8%	17.0%	2.6%	1.7%	0.4%	-	-
30 Hz	87.9%	5.4%	5.4%	0.7%	0.2%	0.1%	0.1%	-
40 Hz	94.3%	2.9%	2.2%	0.4%	0.1%	-	-	-
100 Hz	97.0%	1.9%	0.6%	0.1%	0.2%	-	0.1%	-

with feedback:

freq.	#1	#2	#3	#4	#5	#6	#7	#8
20 Hz	92.0%	1.7%	5.0%	0.4%	0.5%	0.1%	-	-
30 Hz	96.4%	1.5%	1.4%	0.2%	0.2%	0.1%	-	-
40 Hz	97.8%	0.8%	1.0%	0.1%	-	-	-	-
100 Hz	98.3%	1.2%	0.1%	-	0.1%	-	0.1%	-

Table 4.2.2 is similar to Table 4.2.1 except that output levels were taken at 1/2 power, or 60 W continuous.

TABLE 4.2.2 HARMONIC LEVELS AT 1/2 POWER OUTPUT

without feedback:

freq.	#1	#2	#3	#4	#5	#6	#7	#8
20 Hz	55.7%	9.6%	25.7%	4.3%	3.5%	0.6%	0.5%	-
30 Hz	81.2%	7.5%	9.2%	1.1%	0.4%	0.3%	0.2%	-
40 Hz	90.3%	5.0%	3.4%	0.5%	0.5%	0.2%	-	-

with feedback:

freq.	#1	#2	#3	#4	#5	#6	#7	#8
20 Hz	84.7%	2.1%	10.2%	0.8%	1.8%	-	0.3%	-
30 Hz	94.3%	1.4%	2.6%	0.2%	0.6%	-	0.2%	-
40 Hz	94.8%	1.8%	2.2%	-	0.4%	0.6%	-	-

Total harmonic distortion (THD) vs. frequency is given in table 4.2.3. It can be seen that our distortion specifications have been met, as the 1/4 power THD is less than 5% for frequencies 30Hz and above.

TABLE 4.2.3 TOTAL HARMONIC DISTORTION VS. FREQUENCY

freq.	quarter power no feedback:	quarter power with feedback:	half power no feedback:	half power with feedback:
20 Hz	29.6%	8.0%	44.3%	15.3%
30 Hz	12.1%	4.6%	18.8%	5.7%
40 Hz	5.7%	2.2%	9.7%	5.2%
100 Hz	3.0%	1.7%	n.a.	n.a.

4.3 Listening Tests

After completing our system, it was subjected it to extensive listening tests. The system was installed in the audio system at the Computer Music Project, which also happened to be the sight of most of the construction and testing. All who heard the servo system noted substantial improvements both over the previous two-way speaker system and over the uncontrolled subwoofer system.

Test material was carefully chosen for quantity and quality of low-bass information. Switching the accelerometer control into the circuit revealed another dimension in the reproduction of the musical performance, providing a solid foundation and the ability to not only hear, but to feel the music. There is a lot of musical information that much of the public has never heard reproduced through an audio system. Reproducing the full frequency spectrum goes a long way towards bridging the gap between live music and so called 'high-fidelity' systems.

5. CONCLUSION

5.1 Conclusions

It has been demonstrated that by including feedback in the design of an active subwoofer system, high performance results can be obtained without the usual problems of cost and size. The distortion figures and frequency measurements of our completed system have surpassed the specifications claimed, and extended listening has shown that the subwoofer is truly capable of providing low distortion bass down to the lowest audible frequencies. Comparing our results to the only known commercial product of its nature, our design performs very favorably [4].

5.2 Possible Improvements

There was a lot learned in the design, construction, and testing of our servo-controlled subwoofer system. A few improvements were considered that should be incorporated in future versions, should they be built.

First, the sensor and voice-coil should be mechanically coupled using the most rigid method of connection available to the designer. This is a function of both sensor size and shape as well as driver construction. In our case, we mounted the piezo accelerometer on a hard-plastic dustcap, which proved to be a reasonably good solution. However, under extended listening tests with the satellite speakers disconnected, a slight "hoot" or "boom" was noticed which might be attributed to resonances within the dustcap. These are inevitable due to its nonideal rigidity, suggesting two methods of improvement: either the dustcap should be more rigidly reinforced, or the sensor should be relocated.

Another possible improvement follows from the success of the servo control. One of the biggest motivations in building a feedback-controlled design is the reduction in distortion, though distortion only becomes significant at high playback levels. As a result, our system is no longer limited by harmonic distortion at high playback levels, but instead by driver excursion. By using a larger driver, such as a 15 in or an 18 in model, the system would be able to reach much higher

playback levels before excursion limits are reached. The only added cost would be that of buying a larger driver, as all the control electronics would remain essentially the same.

The third and most important improvement starts with the selection of a better sensor. Remember, the sensor's resonances limit the available loop gain that the system can use in minimizing distortion, and using a sensor with resonances placed higher in frequency would allow filter designs that permit more loop gain before the system goes unstable. Using more loop gain also requires that there is more frequency and transient response correction, implying a smaller box size that our design currently uses. Thus, using a large driver in a small box with a higher quality sensor would result in multiple improvements in performance, not to mention a more practical box size.

APPENDIX 2. COMPONENT VALUES

PART	VALUE
R1, R2	10 kΩ
R3	100 kΩ potentiometer
R4, R5, R6, R7	12.5 kΩ
R8	10 kΩ
R9	61.9 kΩ
R10	3.1 kΩ
R11	2.38 kΩ
R12	10 kΩ
R13	3.123 kΩ
R14	5.069 kΩ
R15	25 kΩ trimpot
R16	1.3 kΩ
R17, R18	53.6 kΩ
R19	3.8 MΩ
R20	10 kΩ
R21	7.5 kΩ
R22	4.3 kΩ
R23	650 kΩ
R24, R25	22 MΩ
R26, R27	10 kΩ
R28	4.64 kΩ
R29, R31, R33, R35	90.03 kΩ
R30, R32, R34, R36	180.06 kΩ
C1, C3,	.144 μF
C2, C4	.072 μF
C5	.039 μF
C6	.01 μF
C7	.1 μF
C8	.01 μF
C9, C10, C11, C12	.1 μF
SW1	toggle switch
SW2	roller switch
A1-A5, A7-A8	AD712
A6	AD711

REFERENCES

[1] J. W. Beauchamp, "Theory of Design of Closed Box and Vented Box Loudspeaker Systems," in ECE 303 Course Notes, University of Illinois, Urbana, Illinois, Jan. 1991.

[2] A. E. Brown, "Developing Servo Subwoofers," *Speaker Builder*, pp. 20-31, January 1991.

[3] R. Chalupa, "A Subtractive Implementation of Linkwitz-Riley Crossover Design," *J. Audio Eng. Soc.*, vol 34, no. 7/8, pp. 556-559, July/August 1986.

[4] D. L. Clark, "Equipment Profile: Velodyne ULD-15 Powered Subwoofer," *Audio*, pp. 78-88, November 1987.

[5] V. Dickason, *The Loudspeaker Design Cookbook*, 4th Ed., Peterborough, New Hampshire: Audio Amateur Press, 1991.

[6] R. A. Greiner and Michael Schoessow, "Electronic Equalization of Closed-Box Loudspeakers," *J. Audio Eng. Soc.*, vol 31, no.3, pp. 125-134, March 1983.

[7] W. G. Jung, *IC Op-Amp Cookbook*, 3rd Ed.,Carmel, Indiana: Macmillan, 1991.

[8] S. H. Linkwitz, "Active Crossover Networks for Noncoincident Drivers," *J. Audio Eng. Soc.*, vol. 24, no. 1, pp. 2-8, January/February 1976.

[9] B. D. Smith, "Adjusting Woofers For High Performance," *Speaker Builder*, pp. 22-24, June 1989.

[10] G. W. Tillet, "Motional Feedback in Loudspeakers," *Audio*, pp. 40-43, August 1975.